Journal of Cellular Physiology

Testosterone Abrogates TLR4 Activation in Prostate Smooth Muscle Cells Contributing to the Preservation of a Differentiated Phenotype

CAROLINA LEIMGRUBER, AMADO ALFREDO QUINTAR, LUCIANA NOEMÍ GARCÍA, JUAN PABLO PETITI, ANA LUCÍA DE PAUL AND CRISTINA ALICIA MALDONADO*

Facultad de Ciencias Médicas, Centro de Microscopía Electrónica, Instituto de Investigaciones en Ciencias de la Salud (INICSA-CONICET), Universidad Nacional de Córdoba, Córdoba, Argentina

Prostate smooth muscle cells (pSMCs) are capable of responding to inflammatory stimuli by secreting proinflammatory products, which causes pSMCs to undergo dedifferentiation. Although it has been proposed that androgens decrease proinflammatory molecules in many cells and under various conditions, the role of testosterone in the prostate inflammatory microenvironment is still unclear. Therefore, our aim was to evaluate if testosterone was able to modulate the pSMCs response to bacterial LPS by stimulating primary pSMC cultures, containing testosterone or vehicle, with LPS (1 or 10 μg/ml) for 24–48 h. The LPS challenge induced pSMCs dedifferentiation as evidenced by a decrease of calponin and alpha smooth muscle actin along with an increase of vimentin in a dose-dependent manner, whereas testosterone abrogated these alterations. Additionally, an ultrastructural analysis showed that pSMCs acquired a secretory profile after LPS and developed proteinopoietic organelles, while pSMCs preincubated with testosterone maintained a more differentiated phenotype. Testosterone downregulated the expression of surface TLR4 in control cells and inhibited any increase after LPS treatment. Moreover, testosterone prevented IκB-α degradation and the LPS-induced NF-κB nuclear translocation. Testosterone also decreased TNF-α and IL6 production by pSMCs after LPS as quantified by ELISA. Finally, we observed that testosterone inhibited the induction of pSMCs proliferation incited by LPS. Taken together, these results indicate that testosterone reduced the proinflammatory pSMCs response to LPS, with these cells being less reactive in the presence of androgens. In this context, testosterone might have a homeostatic role by contributing to preserve a contractile phenotype on pSMCs under inflammatory conditions.

J. Cell. Physiol. 9999: 1–10, 2012.

The stroma of the prostate is comprised of the two main cellular components, the fibroblast and smooth muscle cells. By surrounding the glandular acini, the prostatic smooth muscle cells (pSMCs) are strategically located in order to be able to contribute to the complex interactions with the epithelial compartment, thereby maintaining the functionality and structure of the gland (Flickinger, 1972; Farnsworth, 1999). These stromal–epithelial interactions are strictly regulated by testosterone, which induces the secretion of different growth factors that regulate proliferation, differentiation, and cell death acting in a paracrine or autocrine manner (Shaw et al., 2008). In pSMCs, androgens modulate the gene expression of several growth factors, including TGFβ1 and FGF2 (Niu et al., 2003). Moreover, testosterone stimulates in vitro the expression of SMC markers and proliferation of prostate stromal cells (Niu et al., 2001).

The pSMCs are highly responsive cells that exhibit phenotypic changes in response to physiological and pathological modifications in the microenvironment. In particular, pSMCs have been demonstrated to acquire a secretory profile during experimental acute bacterial prostatitis (Quintar et al., 2010). In vitro studies have confirmed that normal rat pSMCs undergo dedifferentiation to a myofibroblast phenotype when they are challenged by bacterial LPS. This pSMC response involves upregulation of TLR4 (Toll-like receptor specific for LPS), the subsequent activation of NF-κB, and secretion of proinflammatory cytokines (Leimgruber et al., 2011). The pSMC phenotypic changes are critical not only because they promote and sustain inflammation, but also because they alter stromal–epithelial interactions (Taboga et al., 2008). As a result, pSMCs have a protagonist role in the development, maintenance, and/or progression of prostatic diseases including prostatitis (Dellabella et al., 2009; Quintar et al., 2010), benign prostate hyperplasia (BPH), (Schauer and Rowley, 2011) and prostate cancer (Tuxhorn et al., 2001; Wong and Tam, 2002; Cunha et al., 2003). For instance, it has been reported that human

Carolina Leimgruber and Amado Alfredo Quintar contributed equally to this work.

The authors of this manuscript have nothing to declare.

Contract grant sponsor: Consejo Nacional de Investigaciones Científicas y Técnicas (CONICET) PIP 2011–2013.
Contract grant sponsor: Secretaría de Ciencia y Tecnología de la Universidad Nacional de Córdoba (SECYT);
Contract grant number: N#169/10.
Contract grant sponsor: FONCYT-ANPCyT;
Contract grant number: PICT#533.

*Correspondence to: Cristina Alicia Maldonado, Facultad de Ciencias Médicas, Centro de Microscopía Electrónica, Universidad Nacional de Córdoba. Pab. Biología Celular 1° piso, Haya de la Torre esq. Enrique Barros, Ciudad Universitaria, X5000HRA Córdoba, Argentina. E-mail: cmaldon@cmefcm.uncor.edu

Manuscript Received: 24 July 2012
Manuscript Accepted: 19 December 2012

Accepted manuscript online in Wiley Online Library (wileyonlinelibrary.com): 00 Month 2012.
DOI: 10.1002/jcp.24314

stromal BPH cells express TLRs for different pathogens and actively contribute to chronic inflammation and prostatic hyperplasia by secreting proinflammatory cytokines and chemokines in response to TLR agonists (Penna et al., 2009).

The role of testosterone in mediating stromal–epithelial interactions motivated us to evaluate its potential in modulating the phenotype of pSMCs and the secretion of inflammatory mediators in response to injuries. Androgens have already been reported to decrease the expression of proinflammatory products in several types of cells and conditions, suggesting that they may exert beneficial effects by modulating inflammatory diseases. In human endothelial cells, dihydrotestosterone might positively affect the progression of atherosclerosis by abrogating the expression of ICAM-1, VCAM-1, IL6, MCP-1, as well as the proteases triggered by TNF-α (Hatakeyama et al., 2002) or LPS (Norata et al., 2006). Testosterone also inhibits IL6 production by fibroblasts (Coletta et al., 2002) and osteoclasts (Hofbauer et al., 1999) induced by proinflammatory factors. In monocyte–macrophages, testosterone not only decreases the synthesis of proinflammatory products including TNF-α and NOS (Rettew et al., 2008), but also enhances anti-inflammatory factors such as IL10 (D'Agostino et al., 1999). Furthermore, androgens ameliorate autoimmune orchitis by reducing the synthesis of MCP-1, TNF-α, and IL-6 in the testes and the secretion of IFN-γ and IL2 by mononuclear cells of the lymph nodes (Fijak et al., 2011).

Although the effects of testosterone on prostate homeostasis and on the inflammatory response in many organs are well known, the role of androgens on the prostate inflammatory microenvironment remains to be elucidated. Accordingly, our aim was to evaluate if testosterone was able to modulate the pSMC response to bacterial LPS in vitro.

Materials and Methods

Animals

Twelve-week-old adult male rats of Wistar strain, weighing 250–350 g, were housed at the Animal Research Facility of the National University of Córdoba in air-conditioned quarters, under a controlled photoperiod (14-h light/10-h darkness) with free access to commercial rodent food and tap water. Animal care and experiments were conducted following the recommendations of the Guidelines of NHI for the Care of and Use of Laboratory Animals, 1996 and approved by a local Institutional committee.

Prostate smooth muscle cell cultures and treatments

Prostate specimens were obtained from six Wistar rats per culture. The cell dissociation and cell cultures have been previously described elsewhere in detail (Leimgruber et al., 2011). Briefly, tissues were minced into small fragments and treated for 30 min with a digestion solution containing 200 U/ml collagenase type IA (Sigma–Aldrich, St. Louis, MO) and 0.05% deoxyribonuclease type I (Sigma–Aldrich, St. Louis, MO) in minimal essential medium SMEM (Sigma). Then, dispersed pSMC cells were washed three times with SMEM, collected by centrifugation for 2 min at 1,000*g* and finally resuspended and adjusted to 1×10^6 cell/ml. Dispersed cells were seeded on 6-well culture plates at a density of 7.5×10^5 cells/well and cultured in the SMC medium MCDB131 (Sigma), supplemented with 10% heat-inactivated fetal calf serum and 10% horse serum (Gibco, Invitrogen, Carlsbad, CA) in a humidified incubator at 37°C supplied with 5% CO_2 in air. The culture medium was replaced daily for 6 days; after which, it was replaced by serum free medium supplemented with 5 μg/ml insulin, 5 μg/ml transferrin, 5 ng/ml selenite, and 2 ng/ml TGFβ1 (Invitrogen). In order to evaluate the influence of androgens on the pSMC inflammatory response, testosterone 10^{-7} M (in ethanol at a final concentration of 0.01%) or its vehicle was added for 48 h before LPS challenge. Finally, the pSMCs were exposed to different doses of LPS (Sigma; 1 or 10 μg/ml) or vehicle for an additional 24 or 48 h.

Electron microscopy

After the treatments described above, the culture media were removed and the pSMCs were fixed for 15 min in Karnovsky mixture containing 1.5% (v/v) glutaraldehyde, 4% (w/v) formaldehyde in 0.1 M cacodylate buffer, pH 7.3, plus 14% sucrose. Then, cell monolayers were scraped from the wells, washed and centrifugated at 1,000*g* for 3 min. Cellular pellets were maintained in Karnovsky mixture for additional 2 h, and then treated with 1% osmium tetroxide for 1 h, dehydrated in a series of graded cold acetones and embedded in Araldite. For ultrastructural studies, 60 nm thin sections were cut with a diamond knife on a Porter-Blum MT2 and JEOL JUM-7 ultramicrotomes, stained with uranyl acetate and lead citrate, and examined in a Zeiss LEO 906E electron microscope and photographed with a Megaview III camera. (Olympus, Center Valley, PA).

Immunofluorescence

Coverslides with pSMC attached cells were fixed with 4% formaldehyde, permeabilized with 0.25% Triton X-100 in PBS and incubated for 1 h in 5% PBS–BSA to block non-specific binding. Slides were incubated overnight at 4°C in a humidified chamber with the following primary antibodies: anti-alpha smooth muscle actin (ACTA2; 1/50 mouse monoclonal, Novocastra, Newcastle, UK), anti-vimentin (1/100 mouse monoclonal, Novocastra), anti-calponin (1/500 mouse monoclonal, Thermo Scientific, Rockford, IL), anti-TLR4 (1/400 polyclonal goat, Santa Cruz Biotechnology, Santa Cruz CA), and anti-p65-NF-κB (1/1,000 rabbit antibody polyclonal, Abcam, Cambridge, MA). Afterwards, the slides were washed three times with PBS and further incubated with Alexa 488 anti-mouse, Alexa 594 anti-goat, or Alexa 594 anti-rabbit secondary antibodies (1/1,000 Invitrogen, Frederick, MD) for 1 h and mounted using fluoromount containing DAPI.

For double immunostaining, slides were labeled for ACTA2 with Alexa 488 anti-mouse as the second antibody, washed, and then incubated with the anti-vimentin antibody using the Alexa 594 anti-mouse as explained above.

To validate the specificity of the immunostaining, controls were performed by applying the same protocol but replacing the primary antibody with 1% PBS–BSA. Images were then obtained using an inverted confocal laser scanning microscope FluoView FV 1000 (Olympus; Tokyo, Japan). Serial z-axis sections were collected with a 40 or 60× objective the analysis of confocal microscopy images was performed using the FV10-ASW 1.6 Viewer software.

Western blotting

The pSMC cultures were washed with ice-cold PBS and harvested in 120 μl cold PBS containing 1.25% Igepal CA-630, 1 mM EDTA, 2 mM PMSF, 10 μg/ml leupeptin, and 10 μg/ml aprotinin. The lysate was centrifuged at 14,000*g* for 20 min at 4°C to pellet the Igepal CA-630-insoluble material and the supernatant was stored in aliquots frozen at −80°C until required. The total protein concentration was measured with a Bio-Rad kit (Bio-Rad Laboratories, Hercules, CA). Denatured protein samples (30 μg/lane) were then separated on 12% SDS–polyacrylamide gel and blotted onto a Hybond-C membrane (Amersham Pharmacia, Buckinghamshire, UK) with incubation steps being performed in 5% defatted dry milk in PBS/0.1% Tween 20. Membranes were rinsed and incubated for 3 h with a goat polyclonal antibody diluted 1/400, which recognizes TLR4 (Santa Cruz), 1/200 mouse anti-ACTA2 (Novocastra), 1/300 mouse anti-Vimentin (Novocastra), 1/500 mouse anti-calponin (Thermo Scientific) 1/400 anti-IκB-α (Santa Cruz), 1/700 anti-p-ERK (Sigma), and anti-total ERK (Santa Cruz). After washing, the blots were incubated with a peroxidase-conjugated (HRP) bovine anti-goat (Santa Cruz), goat anti-rabbit (Santa Cruz), or goat anti-mouse (Jackson Immunoresearch, West

Grove, PA) secondary antibody, and revealed with an Enhanced Chemiluminescence detection system (ECL, Amersham Biosciences, Buckinghamshire, UK) following the manufacturer's instructions. Emitted light was captured on Hyperfilm (Amersham Pharmacia) and densitometry analysis was performed by applying the Scion Image software (V. beta 4.0.2, Scion Image Corp., Frederick, MD). The relative expression was compared among different treatments by taking the control group value as a reference. The expression of ACTB (1/5,000 monoclonal anti-α actin; Sigma) was used as an internal control to confirm equivalent total protein loading.

Elisa

In order to quantify TNF-α and IL6 secretion by pSMC, 1 ml of medium was collected from the plates, centrifuged at 4°C at 1400 rpm for 15 min and stored at −20°C until the day of the assay. The secretion was measured by commercially available sandwich ELISA kits (eBioscience, San Diego, CA for TNF-α and BD Biosciences, Franklin Lakes, NJ for IL6), according to the manufactureŕs instructions.

Flow cytometry

Living control and treated pSMCs were detached by trypsinization. For detection of surface TLR4, 1×10^5 cells were incubated overnight with a goat polyclonal antibody diluted 1/400 anti-TLR4 (Santa Cruz) and then with an Alexa 488-conjugated antibody (1/1,000; Invitrogen). All the washing steps and the incubations were performed using a buffer containing 2% fetal bovine with the double purpose of protecting the cells and blocking non-specific labeling. Controls were performed by using cells incubated with the secondary antibody omitting the primary antibody or replacing the anti-TLR4 antibody by a purified non-reactive goat IgG (Santa Cruz). Then, the cells were washed, resuspended in filtered PBS, and analyzed with a Cytoron Absolute Flow Cytometer (Ortho Diagnostic System, Raritan, NJ), and the fluorescence was analyzed with Flowjob software (Tree Star, Inc., Ashland, OR).

Proliferation assay

The pSMCs were stimulated with LPS for 24 h, with BrdU (3 mg/ml) being added to the culture medium 3 h before finishing the protocols. The cells attached to the coverslips were fixed with 4% formaldehyde in PBS for 30 min at room temperature, washed in PBS, and permeabilized with 0.5% Triton X-100 for 10 min. Non-specific immunoreactivity was blocked with 1% PBS–BSA for 30 min at RT, and the cells were incubated overnight with a monoclonal antibody against BrdU (Amersham Pharmacia) at 4°C in a wet chamber. After washing in PBS, the cells were incubated with a biotinylated anti-mouse IgG diluted 1/100 (GE Healthcare, Buenos Aires, Argentina). The coverslips were washed again with PBS, and the pSMCs were incubated with the avidin–biotinperoxidase complex (ABC; Vector; Burlingame, CA). The immunoreactivity for BrdU was visualized with 3,3-diaminobenzidine tetrahydrochloride (DAB) as a chromogen. A total of 1,000 immunoreactive cells were examined by light microscopy in randomly chosen fields of each glass slide, in order to establish the percentage of BrdU immunoreactive cells. Three slides were analyzed for each group, derived from the same cell preparations. Experiments were replicated at least three times with separate batches of cell preparations.

Statistical analysis

Data from more than two groups were analyzed using analysis of variance (ANOVA) with Tukey as the post-test. Statistical testing and calculation of Western blot data were performed using the InStat V2.05 software from GraphPad, Inc.

Results

Testosterone inhibited the LPS-induced TLR4 increase

By Western blot, the expression of TLR4 in pSMCs exhibited a significant increase after LPS treatment for both doses tested compared with control pSMCs (Fig. 1A,B). When testosterone was added to the incubation medium, the TLR4 signal was similar to control cells. This observation was confirmed by immunofluorescence, which showed a strong reactivity in LPS-treated pSMCs compared to control cells (Fig. 1C). In contrast, when cells were cultured in medium supplemented with testosterone, the TLR4 increase triggered by LPS was not observed (Fig. 1C).

Considering that LPS stimulation induces TLR4 internalization in immune cells (Saitoh, 2009), we analyzed the effects of testosterone on cell surface TLR4 after LPS treatment as a parameter of receptor activation. By flow cytometry (Fig. 1D), in controls, only a low percentage of pSMCs was observed to exhibit surface TLR4 ($8.45 \pm 1.71\%$), which was even lower in the presence of testosterone ($6.09 \pm 0.03\%$ $P < 0.05$ vs. control). As expected, after 60 min of LPS, the percentage of surface TLR4 in pSMCs decreased as compared with control cells ($4.92 \pm 0.41\%$ $P < 0.01$ vs. control). This effect was not observed when cells were triggered in the presence of testosterone plus LPS ($6.51 \pm 0.43\%$).

Testosterone decreased NF-κB activation and cytokine secretion stimulated by LPS

The recognition of LPS by TLR4 initiates a signaling pathway that culminates with the translocation of NF-κB to the nucleus, thereby activating several genes associated to the inflammatory response. Here, we characterized the effects of testosterone on LPS-induced NF-κB activation by evaluating the localization of the p65-subunit by immunofluorescence. Controls exhibited $5 \pm 0.40\%$ of cells with nuclear NF-κB, and pSMCs cultured in presence of testosterone showed a similar basal level ($4.5 \pm 2.76\%$). As expected, the LPS treatment induced NF-κB traslocation, resulting in a maximum of $21 \pm 4.16\%$ positive cells at 15 min. Notably, preincubation with testosterone decreased LPS-induced nuclear NF-κB to $7.5 \pm 3.01\%$ at 15 min, and the maximum was observed at 30 min after stimulus with only a $12 \pm 5.24\%$ of positive cells (Fig. 2A). In addition, we studied the kinetics of IκB-α degradation, which is an inhibitory protein that retains NF-κB in the cytoplasm. As shown in Figure 2B, LPS promoted IκB-α degradation in the pSMCs, starting at 15 min and being more evident at 30 min. In the presence of testosterone, IκB-α degradation started slightly later and was observed only 30 min after LPS treatment, which was correlated with the highest NFκB traslocation levels in this group. After 120 min, IκB-α was resynthesized in both with testosterone or vehicle groups.

In addition, the secretion of pro-inflammatory cytokines was also quantified as part of the TLR4 pathway activation by LPS and its modulation by testosterone. The pSMCs increased the levels of the pro-inflammatory cytokines TNF-α and IL6 after an LPS treatment at 24 or 48 h, thus confirming previous results (Leimgruber et al., 2011). Interestingly, pSMCs cultured in presence of the androgen secreted significantly lower amounts of TNF-α and IL6 after an LPS challenge, at both doses and times tested (Fig. 3A,B).

Testosterone contributed to maintaining a more differentiated phenotype after LPS stimulation

The phenotype of pSMCs was assessed by transmission electron microscopy as well as by immunostaining of specific markers. At the ultrastructural level, control cells displayed scarce perinuclear organelles, mainly consisting of high electron-dense mitochondria and rough endoplasmic reticulum (RER) cisternae, and a well-developed contractile apparatus

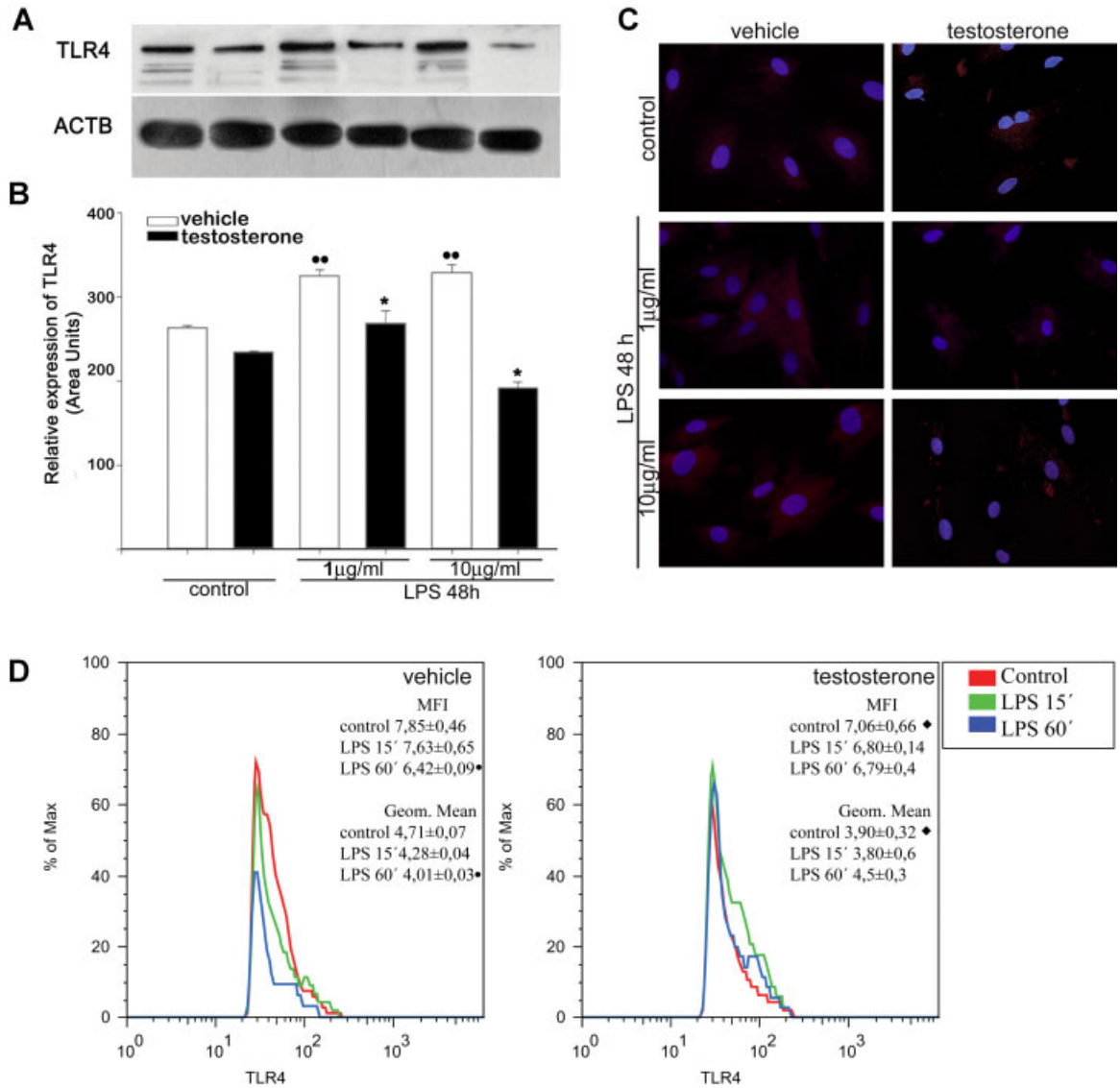

Fig. 1. Influence of testosterone on TLR4 expression. Cells treated with LPS 48 h, in medium containing testosterone (10^{-7} M) or its vehicle, were analyzed by Western blot (A, B) and immunofluorescence (C); both reveal that testosterone significantly prevented the increase in TLR4 induced by LPS. The analysis of superficial TLR4 by flow citometry (D) shows that LPS (1 µg/ml) induced internalization of TLR4 at 15 min and more remarkable at 60 min, which was partially inhibited by testosterone (10^{-7} M). Mean fluorescence intensity (MFI) and geometric mean were calculated as parameters of intensity levels. The Western blot values were normalized with ACTB expression and represent the mean ± SE of five independent protocols. $^{**}P < 0.01$ versus vehicle control; $^{*}P < 0.05$ versus vehicle control; ~~rhombus~~ $P < 0.05$ versus vehicle control; $^{*}P < 0.05$ versus LPS + vehicle, ANOVA-Tukey.

corresponding to a smooth muscle phenotype (Fig. 4A); pSMCs preincubated with testosterone also showed similar features (Fig. 4B). When pSMCs were treated with LPS, they underwent hypertrophy with an increased cytoplasmic/nuclear area, exhibiting numerous RER cisternae, and a well-developed golgi complex, as well as mitochondria with a lower electron-density (Fig. 4C,E). Meanwhile, contractile filaments were scarcely seen and most cells presented a very low density extracellular matrix around the plasma membrane (Fig. 4C,E). Interestingly, in pSMCs cultured with testosterone, the cellular hypertrophy was lower after LPS, with cells conserving a more-differentiated smooth muscle phenotype, even at the higher concentration of LPS (Fig. 4D,F).

The expression of ACTA2 and calponin as SMC markers and vimentin as a fibroblast marker was analyzed by IF and Western blot. Control cells, both incubated with testosterone or vehicle, showed intense ACTA2 and calponin expression by IF, and were negative for vimentin (Fig. 5D,E). After LPS challenge, pSMCs displayed disorganized ACTA2 filaments, weak calponin expression, and a simultaneous induction of vimentin (Fig. 5D,E). In contrast, testosterone reduced these effects in LPS-treated pSMCs. By Western blot, at both LPS doses evaluated, testosterone modulation on LPS effects was clearly verified for the higher 10 µg/ml LPS concentration, with testosterone contributing to maintain ACTA2 and calponin expression and to prevent vimentin increase, both at 24 and

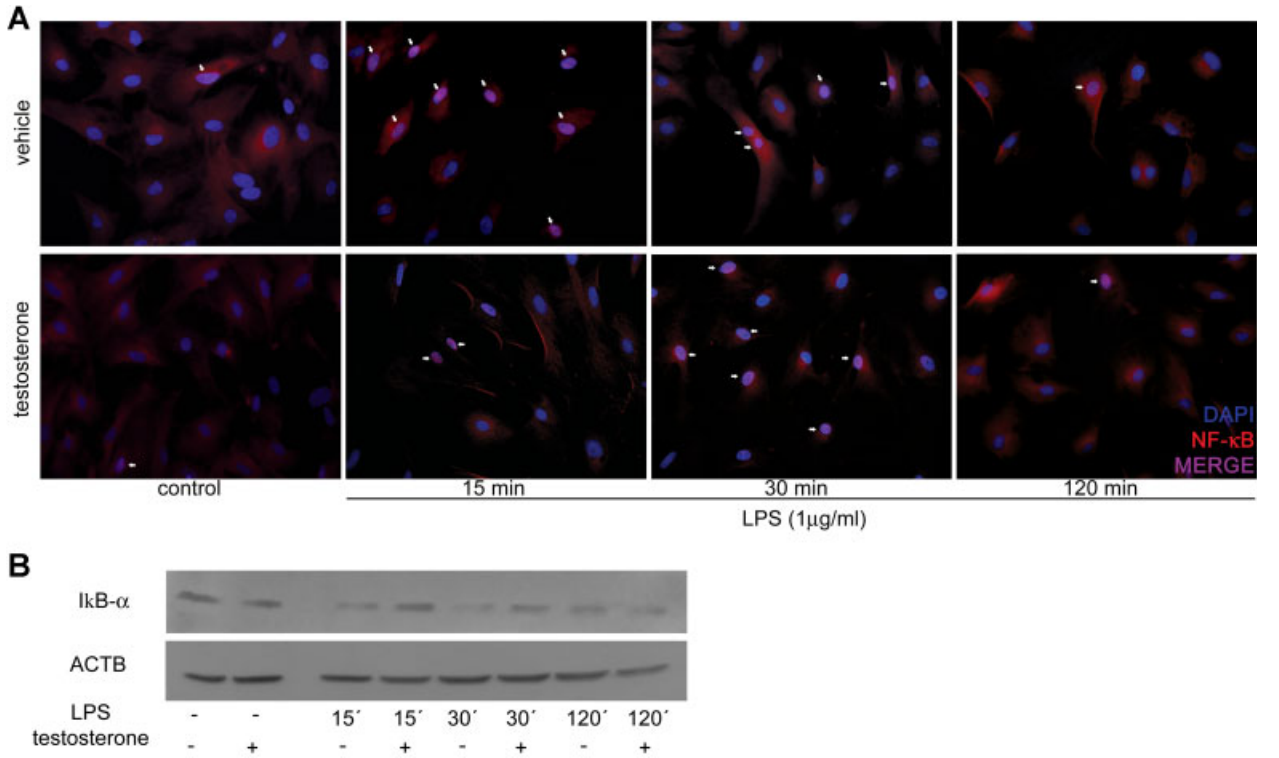

Fig. 2. Effect of testosterone on NF-κB activity after LPS. By immunofluorescence (A) LPS incited NF-κB nuclear traslocation visualized by the colocalization of p65 subunit (red) and DAPI (blue) signals, producing purple fluorescence (arrows). Testosterone reduced the LPS-induced NF-κB traslocation in medium without androgens. The experiment was performed three times, and the pictures correspond to a representative field for each time period studied. IκB-α expression in pSMCs by Western blot (B) demonstrating a rapid degradation of this kinase at 15 min after LPS stimulation. Preincubation with testosterone inhibited IκB-α degradation, which was seeing at 30 min after an LPS challenge. Original magnification 40×.

48 h (Fig. 5A–C). For the lower LPS concentration (1 μg/ml), testosterone only succeeded to modulate ACTA2 and vimentin changes within the first 24 h of treatment. Taken together, these data indicate that testosterone reduced the LPS-induced dedifferenciation of pSMCs.

Testosterone eliminated the proliferation of pSMCs induced by LPS

As part of the phenotypical changes triggered by LPS, the pSMCs underwent cellular proliferation as assessed by BrdU incorporation, thus corroborating previous results. When pSMCs were exposed to testosterone, a significant increase of BrdU positive cells was detected compared to control cells (Fig. 6A), which was consistent with the trophic effect of testosterone on pSMCs (Welsh et al., 2011). In addition, pSMCs cultured with testosterone and stimulated with LPS displayed a significantly decrease in the proliferation rate compared to LPS plus vehicle (Fig. 6A). We next analyzed, at protein level, ERK1/2 activation which is associated with cell proliferation, and pSMCs incubated with testosterone supplemented medium showed a higher expression of p-ERK1/2 than control pSMCs (Fig. 6B). Finally, LPS promoted ERK1/2 phosphorylation with a peak occurring at 5 min, but the presence of testosterone was observed to half this activation (Fig. 6B).

Discussion

The role of prostatic resident cells in immune/inflammatory processes within the gland is just starting to be revealed. Recent reports indicate that pSMCs may represent a main player in the inflammatory microenvironment present in prostate diseases (Birbach et al. 2011; Chughtai et al., 2011). Strikingly, however, the influence of androgens on the pSMCs response to proinflammatory stimuli has not yet been elucidated. Our work addressed for the first time the effects of testosterone on the pSMC response to LPS in vitro, isolated from professional immune cells, demonstrating that androgens reduced TLR4 stimulation and NF-κB activation, and led to a lower secretion of proinflammatory cytokines against LPS. Furthermore, the presence of testosterone reduced the synthesis of extracellular matrix and maintained a more differentiated pSMC phenotype, suggesting that androgens have a homeostatic role in the regulation of inflammatory processes incited by pSMCs.

Experimental studies have documented that prostate stromal cells can initiate in vitro a proinflammatory response by activation of the TLRs present in these cells (Penna et al., 2009; Leimgruber et al., 2011). This fact reveals that stromal cells are able to sense pathogens and danger signals from the microenvironment. Related to this, we previously reported that pSMCs express TLR4, being dedifferentiated and activated after LPS treatment and thereby stimulating the expression of proinflammatory genes via nuclear translocation of NFκB (Leimgruber et al., 2011). Although the phenotypic changes of pSMCs after LPS might be interpreted as a defensive mechanism, the consequences of the inflammatory amplification generated by SMCs could be dangerous for the reproductive functions.

In the prostate gland, testosterone may control inflammation by maintaining a high expression of anti-inflammatory epithelial

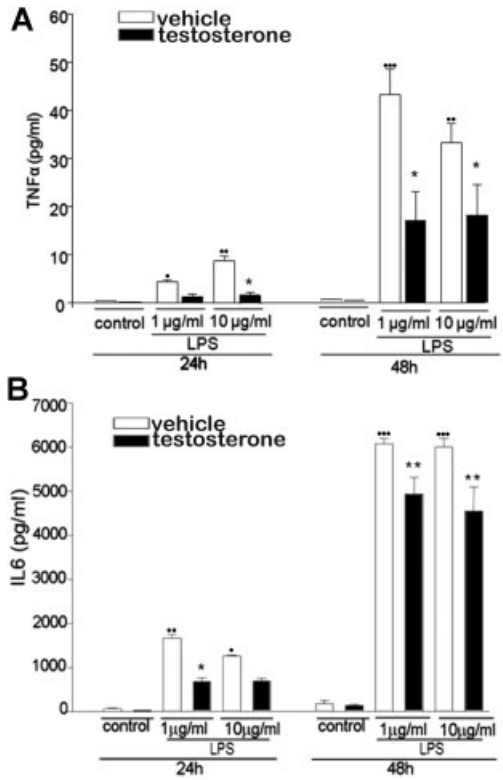

Fig. 3. Testosterone diminished the cytokine production induced by LPS. TNF-α (A) and IL6 (B) secretion were measured by ELISA in supernatants of pSMCs. Both, cytokines levels were lower in the presence of testosterone, with significant differences observed at 48 h of treatment for both LPS doses evaluated. Data refer to mean ± SE from three independent experiments. *$P < 0.05$ versus LPS + vehicle, **$P < 0.01$ versus LPS + vehicle; •$P < 0.05$ versus vehicle control; ••$P < 0.01$ versus vehicle control; •••$P < 0.001$ versus vehicle control. ANOVA-Tukey.

molecules such as prostatic binding protein (PBP), a secretory protein that inhibits macrophage activity (Maccioni et al., 2001) and thus contributes to protect male gametes in semen. In agreement, it has been previously reported that testosterone reduces the infiltration of inflammatory cells and decreases the proinflammatory profile in a model of prostate inflammation associated with metabolic syndrome (Vignozzi et al., 2012). Furthermore, androgen depletion in humans has been shown to induce an important recruitment of immune cells to the prostate (Mercader et al., 2001). However, there is no evidence revealing how testosterone regulates immune responses or which cells are the responsible for this modulation within the prostate gland.

In the present study, we have demonstrated that pSMCs, isolated from both epithelial and immune cells, are main targets of the anti-inflammatory ability of testosterone, which appeared to inhibit different downstream points of the TLR4 pathway. Under basal conditions testosterone downregulated the expression of surface TLR4, making the pSMCs less responsive to bacterial or danger signals from the microenvironment, and testosterone also prevented the increase of TLR4 expression after LPS treatment compared with controls. In addition, testosterone inhibited IκB-α degradation, a protein that sequestrates NF-κB into the cytoplasm, thereby preventing its translocation to the nucleus after stimulation. Consequently, testosterone decreased the LPS-incited NF-κB activation, leading to a reduction in the cytokine production by pSMCs in the presence of androgens (Fig. 7). A similar finding was previously reported in LNCaP cancer cells, where 5α-dihydrotestosterone inhibited NF-κB-mediated gene activation of IL6 by maintaining the levels of IκB-α (Keller et al., 1996), indicating that this signaling pathway is strongly implicated in the anti-inflammatory effects of androgens in the prostate gland.

Androgens have been reported to control the activation of proinflammatory cascades in some other types of cells. For instance, macrophages cultured in the presence of testosterone display a low expression of TLR4 and a reduced production of proinflammatory cytokines after LPS compared to non-treated cells (Rettew et al., 2008). Similar results were reported in non-professional immune cells such as endothelial cells, where dihydrotestosterone inhibited the LPS-triggered increase of TLR4 and cytokine release (Norata et al., 2006). Moreover, it has been previously demonstrated that testosterone reduces the vascular cell adhesion molecule-1 induced by TNF-α by down-regulating the NF-κB activity in human endothelial cells (Hatakeyama et al., 2002). In the prostate gland, a very recent article has suggested that in vivo testosterone negatively modulates the TLR4 pathway, including the expression of TLR4, CD14, and MyD88 (Quintar et al., 2012). Our results show that pSMCs are regulated in vitro in a similar way.

The pSMCs are strongly involved in the pathogenesis of all prostatic disorders by secreting inflammatory factors that maintain a persistent activation of a proinflammatory microenvironment where pSMCs can undergo dedifferentiation to a secretory profile, which finally leads to a repeated exacerbated inflammation. This has been demonstrated, for example, in an acute model of bacterial prostatitis, where pSMCs were shown to acquire a secretory phenotype (Quintar et al., 2010), with this phenotypic change being corroborated in vitro by stimulating pSMCs with LPS (Leimgruber et al., 2011). Furthermore, the proinflammatory cytokines IL8 has been demonstrated in vitro to induce a myofibroblastic phenotype in prostate stromal cells (Schauer et al., 2008). In the present study, we have demonstrated that testosterone promotes a lower secretion of cytokines after LPS challenge, which was associated to a more-differentiated profile in pSMC, indicating that androgens might indirectly modulate the status of pSMC differentiation by maintaining a controlled proinflammatory microenvironment after pathogen invasion.

As part of the investigations into the modulation exerted on pSMC phenotype by testosterone, we also evaluated the effect on cell proliferation activated after LPS challenge as we previously demonstrated. In agreement with the results of other authors (Nheu et al., 2011; Niu et al., 2001), unstimulated pSMCs displayed a higher proliferation rate in the presence of testosterone, which occurred together with an increase of p-ERK1/2. Interestingly, testosterone eliminated the mitogenic effect of LPS on pSMCs as well as the early phosphorylation of ERK1/2. Surprisingly, the proliferation was lower than in the controls, and this strengthened proliferative inhibition triggered by testosterone may have been a consequence of the cross-talk between LPS signaling and the androgen receptor. Regarding this, it has been described that NF-κB p65 physically interacts with steroid hormone receptors and that interaction was sufficient to transrepress each steroid receptor (McKay and Cidlowski, 1998). Finally, the contribution of other signaling cascades, such as PI3 kinase/AKT pathway in the testosterone effect on pSMC cannot be discarded (Kang et al., 2004; Yu et al., 2010).

Summing up, our findings have revealed homeostatic effects of androgens on pSMCs that included the modulation of pSMC responsiveness to inflammatory stimuli and the control of

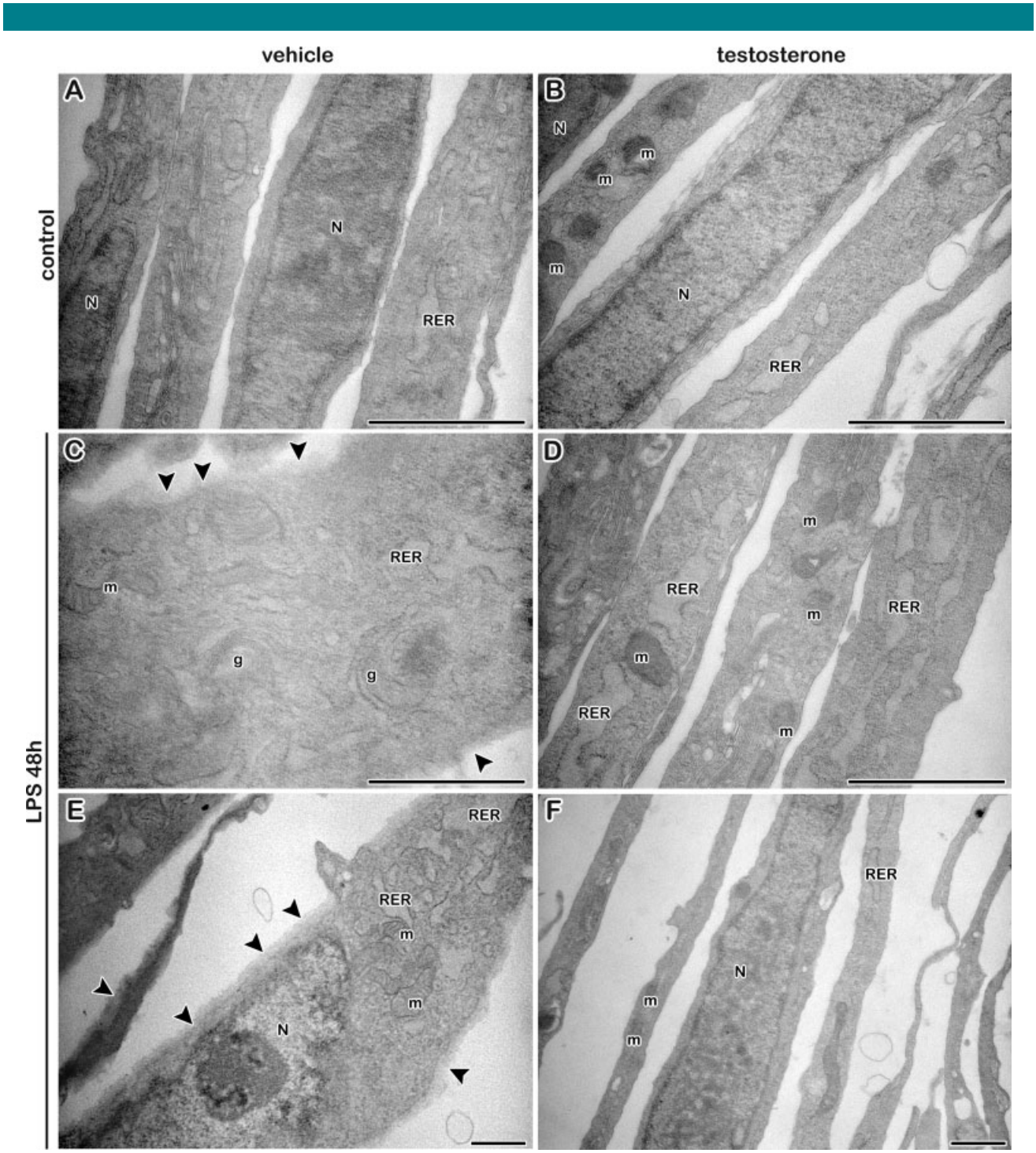

Fig. 4. Ultrastructural features of pSMCs. The pSMC in both controls (A and B) are thin and contain electron-dense mitochondria (m) and some dilated RER cisternae and contractile filaments. After LPS, cells appear hypertrophied and exhibit numerous organelles as low electron-dense mitochondria, well-developed golgi complexes (g) and dilated RER cisternae with secretory content, and a thick extracellular matrix (arrowheads) surrounding the cells (C and E). In the presence of testosterone, pSMCs display similar morphological pattern to their controls (D and F). N, nucleus. Bar, 1 μm.

persistent proinflammatory mediators in the prostate. In addition, androgens were demonstrated to preserve a normal phenotype on pSMCs, thus preventing alterations taking place in the epithelial–stromal interactions. Finally, the actions of testosterone as an anti-inflammatory factor in the prostate represent a key aspect in the physiology and pathophysiology of the gland, considering that the inflammatory processes need to be strictly controlled in the male tract to protect the gametes.

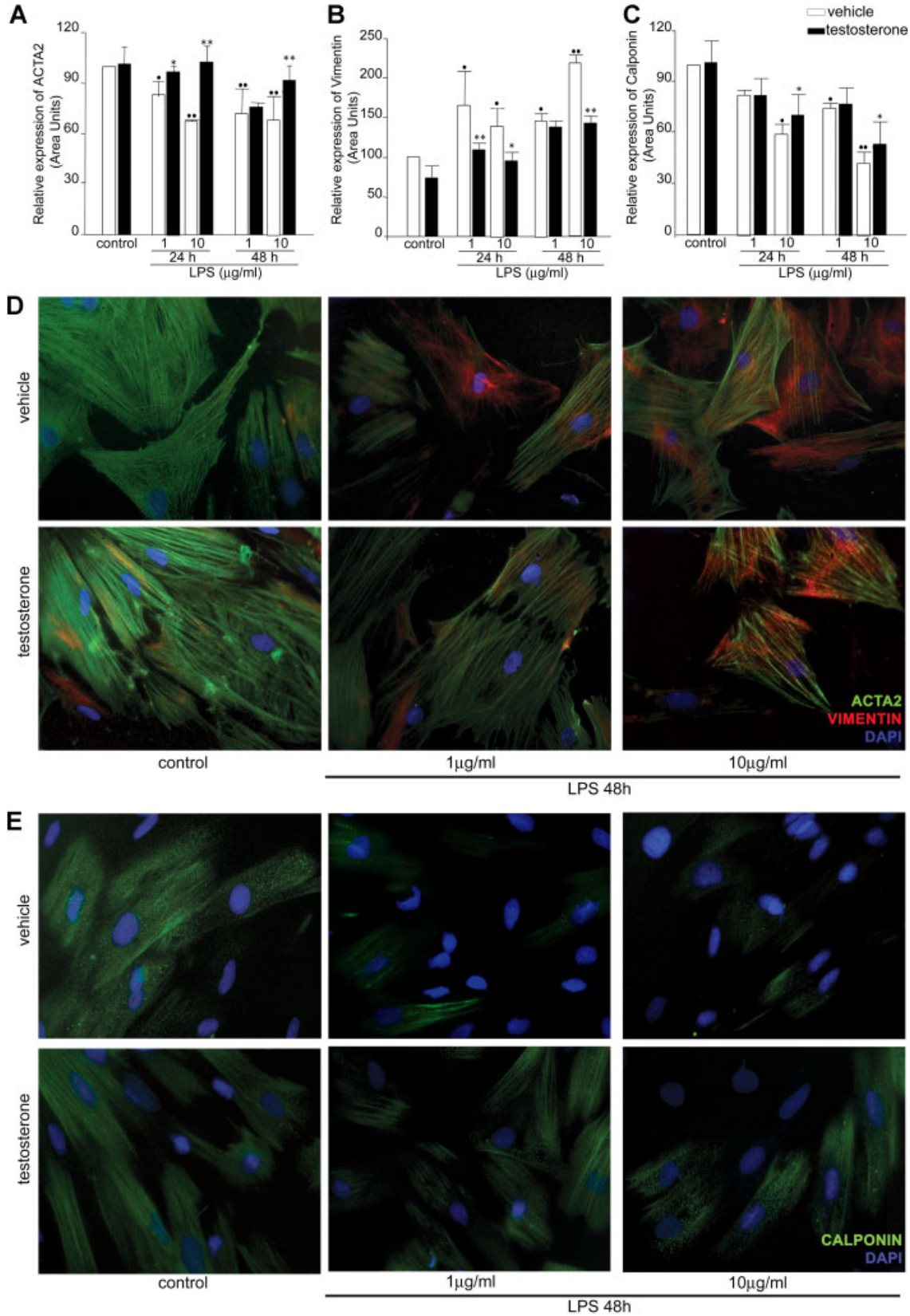

Fig. 5. Influence of testosterone on the pSMC phenotypical *status*. Using Western blot (A–C) and immunofluorescence (D and E), LPS, at both doses and times evaluated, was shown to induce a decrease in the ACTA2 (A and D) and calponin (C and E) expressions at 24 h, which was intensified at 48 h after LPS along with an increase in vimentin content (B and D). The differentiation marker changes induced by LPS were avoided by testosterone. Nuclei were counterstained with DAPI. The Western blot values were normalized with ACTB expression, and represent the mean of the cultures per group obtained from three independent protocols. $^{*}P < 0.05$ versus LPS + vehicle, $^{**}P < 0.01$ versus LPS + vehicle; $^{\bullet}P < 0.05$ versus vehicle control; $^{\bullet\bullet}P < 0.01$ versus vehicle control. ANOVA-Tukey. Original magnification 60×.

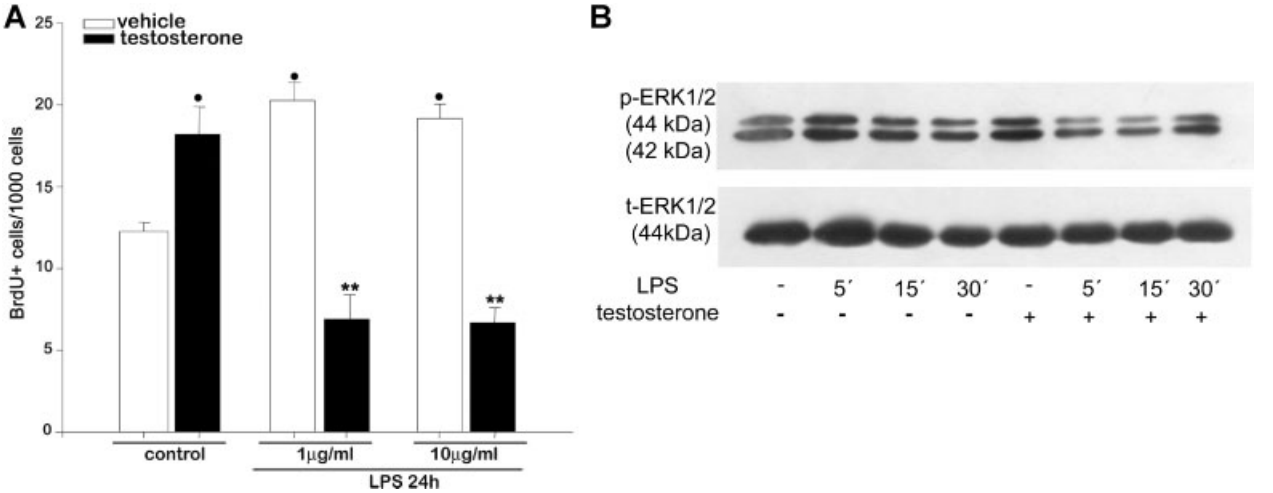

Fig. 6. Analysis of the proliferative rate of pSMCs. By using BrdU incorporation (A), LPS significantly increased cell proliferation, at both doses analyzed, compared with its control. Although, in basal conditions pSMC proliferation was significantly higher in the presence of testosterone (10^{-7} M), the androgen inhibited the LPS-induced proliferation. ERK phosphorylation was assessed by Western blot (B) as a proliferation-associated cascade, which exhibited an increased at 5 and 15 min after LPS (1 μg/ml). Testosterone abrogated this ERK activation. $^{*}P < 0.05$ versus vehicle control; $^{**}P < 0.01$ versus LPS + vehicle. ANOVA-Tukey.

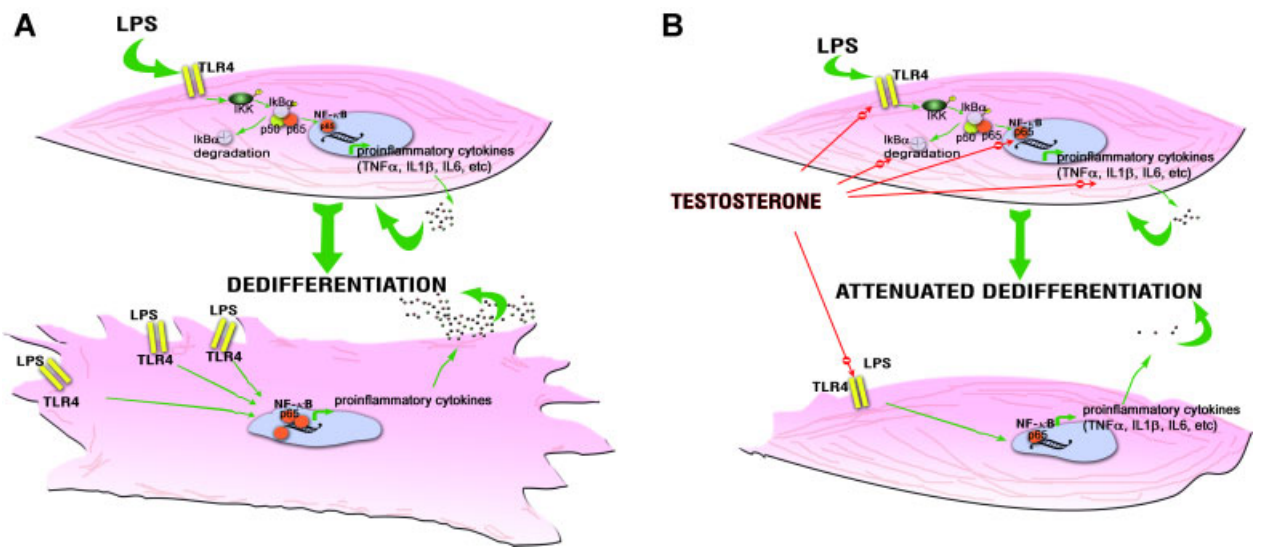

Fig. 7. Role of testosterone on the pSMC response to bacterial LPS. A: The recognition of LPS by TLR4 induces the phosphorylation and degradation of the IκB complex, with the subsequent translocation of NFκB to the nucleus and the expression of several proinflammatory genes. This proinflammatory microenvironment incites the dedifferentiation of pSMC and the acquisition of a myofibroblast phenotype. B: Testosterone negatively regulates different points of the TLR4 signaling pathway, including surface TLR4, IκBα degradation and NFκB translocation turning the cells less-responsive.

Acknowledgments

We gratefully acknowledge the excellent technical assistance of Mercedes Guevara, Elena Pereyra, Cristian Giacomelli, and Lucia Artino. We also thank Cecilia Sampedro for help us in fluorescence imaging. Thanks are due to Team-18 and C7 for their constant advice. We would also like to thank native speaker Dr. Paul Hobson for revision of the manuscript.

Literature Cited

Birbach A, Eisenbarth D, Kozakowski N, Ladenhauf E, Schmidt-Supprian M, Schmid JA. 2011. Persistent inflammation leads to proliferative neoplasia and loss of smooth muscle cells in a prostate tumor model. Neoplasia 13:692–703.

Chughtai B, Lee R, Te A, Kaplan S. 2011. Inflammation and benign prostatic hyperplasia: Clinical implications. Curr Urol Rep 12:274–277.

Coletta RD, Reynolds MA, Martelli-Junior H, Graner E, Almeida OP, Sauk JJ. 2002. Testosterone stimulates proliferation and inhibits interleukin-6 production of normal and hereditary gingival fibromatosis fibroblasts. Oral Microbiol Immunol 17:186–192.

Cunha GR, Hayward SW, Wang YZ, Ricke WA. 2003. Role of the stromal microenvironment in carcinogenesis of the prostate. Int J Cancer 107:1–10.
D'Agostino P, Milano S, Barbera C, Di Bella G, La Rosa M, Ferlazzo V, Farruggio R, Miceli DM, Miele M, Castagnetta L, Cillari E. 1999. Sex hormones modulate inflammatory mediators produced by macrophages. Ann N Y Acad Sci 876:426–429.
Dellabella M, Milanese G, Sigala S, d'Anzeo G, Arrighi N, Bodei S, Muzzonigro G. 2009. The role of the prostatic stroma in chronic prostatitis/chronic pelvic pain syndrome. Inflamm Res 58:829–836.
Farnsworth WE. 1999. Prostate stroma: Physiology. Prostate 38:60–72.
Fijak M, Schneider E, Klug J, Bhushan S, Hackstein H, Schuler G, Wygrecka M, Gromoll J, Meinhardt A. 2011. Testosterone replacement effectively inhibits the development of experimental autoimmune orchitis in rats: Evidence for a direct role of testosterone on regulatory T cell expansion. J Immunol 186:5162–5172.
Flickinger CJ. 1972. The fine structure of the interstitial tissue of the rat prostate. Am J Anat 134:107–125.
Hatakeyama H, Nishizawa M, Nakagawa A, Nakano S, Kigoshi T, Uchida K. 2002. Testosterone inhibits tumor necrosis factor-alpha-induced vascular cell adhesion molecule-1 expression in human aortic endothelial cells. FEBS Lett 530:129–132.
Hofbauer LC, Ten RM, Khosla S. 1999. The anti-androgen hydroxyflutamide and androgens inhibit interleukin-6 production by an androgen-responsive human osteoblastic cell line. J Bone Miner Res 14:1330–1337.
Kang HY, Cho CL, Huang KL, Wang JC, Hu YC, Lin HK, Chang C, Huang KE. 2004. Nongenomic androgen activation of phosphatidylinositol 3-kinase/Akt signaling pathway in MC3T3-E1 osteoblasts. J Bone Miner Res 19:1181–1190.
Keller ET, Chang C, Ershler WB. 1996. Inhibition of NFkappaB activity through maintenance of IkappaBalpha levels contributes to dihydrotestosterone-mediated repression of the interleukin-6 promoter. J Biol Chem 271:26267–26275.
Leimgruber C, Quintar AA, Sosa LD, Garcia LN, Figueredo M, Maldonado CA. 2011. Dedifferentiation of prostate smooth muscle cells in response to bacterial LPS. Prostate 71:1097–1107.
Maccioni M, Riera CM, Rivero VE. 2001. Identification of rat prostatic steroid binding protein (PSBP) as an immunosuppressive factor. J Reprod Immunol 50:133–149.
McKay LI, Cidlowski JA. 1998. Cross-talk between nuclear factor-kappa B and the steroid hormone receptors: Mechanisms of mutual antagonism. Mol Endocrinol 12:45–56.
Mercader M, Bodner BK, Moser MT, Kwon PS, Park ES, Manecke RG, Ellis TM, Wojcik EM, Yang D, Flanigan RC, Waters WB, Kast WM, Kwon ED. 2001. T cell infiltration of the prostate induced by androgen withdrawal in patients with prostate cancer. Proc Natl Acad Sci USA 98:14565–14570.
Nheu L, Nazareth L, Xu GY, Xiao FY, Luo RZ, Komesaroff P, Ling S. 2011. Physiological effects of androgens on human vascular endothelial and smooth muscle cells in culture. Steroids 76:1590–1596.
Niu Y, Xu Y, Zhang J, Bai J, Yang H, Ma T. 2001. Proliferation and differentiation of prostatic stromal cells. BJU Int 87:386–393.
Niu YJ, Ma TX, Zhang J, Xu Y, Han RF, Sun G. 2003. Androgen and prostatic stroma. Asian J Androl 5:19–26.
Norata GD, Tibolla G, Seccomandi PM, Poletti A, Catapano AL. 2006. Dihydrotestosterone decreases tumor necrosis factor-alpha and lipopolysaccharide-induced inflammatory response in human endothelial cells. J Clin Endocrinol Metab 91:546–554.
Penna G, Fibbi B, Amuchastegui S, Cossetti C, Aquilano F, Laverny G, Gacci M, Crescioli C, Maggi M, Adorini L. 2009. Human benign prostatic hyperplasia stromal cells as inducers and targets of chronic immuno-mediated inflammation. J Immunol 182:4056–4064.
Quintar AA, Doll A, Leimgruber C, Palmeri CM, Roth FD, Maccioni M, Maldonado CA. 2010. Acute inflammation promotes early cellular stimulation of the epithelial and stromal compartments of the rat prostate. Prostate 70:1153–1165.
Quintar AA, Leimgruber C, Pessah OA, Doll A, Maldonado CA. 2012. Androgen depletion augments antibacterial prostate host defences in rats. Int J Androl 35:845–859.
Rettew JA, Huet-Hudson YM, Marriott I. 2008. Testosterone reduces macrophage expression in the mouse of toll-like receptor 4, a trigger for inflammation and innate immunity. Biol Reprod 78:432–437.
Saitoh S. 2009. Chaperones and transport proteins regulate TLR4 trafficking and activation. Immunobiology 214:594–600.
Schauer IG, Rowley DR. 2011. The functional role of reactive stroma in benign prostatic hyperplasia. Differentiation 82:200–210.
Schauer IG, Ressler SJ, Tuxhorn JA, Dang TD, Rowley DR. 2008. Elevated epithelial expression of interleukin-8 correlates with myofibroblast reactive stroma in benign prostatic hyperplasia. Urology 72:205–213.
Shaw A, Attia S, Bushman W. 2008. Prostate stromal and urogenital sinus mesenchymal cell lines for investigations of stromal–epithelial interactions. Differentiation 76:599–605.
Taboga SR, Scortegagna E, Siviero MP, Carvalho HF. 2008. Anatomy of smooth muscle cells in nonmalignant and malignant human prostate tissue. Anat Rec (Hoboken) 291:1115–1123.
Tuxhorn JA, Ayala GE, Rowley DR. 2001. Reactive stroma in prostate cancer progression. J Urol 166:2472–2483.
Vignozzi L, Morelli A, Sarchielli E, Comeglio P, Filippi S, Cellai I, Maneschi E, Serni S, Gacci M, Carini M, Piccinni MP, Saad F, Adorini L, Vannelli GB, Maggi M. 2012. Testosterone protects from metabolic syndrome-associated prostate inflammation: An experimental study in rabbit. J Endocrinol 212:71–84.
Welsh M, Moffat L, McNeilly A, Brownstein D, Saunders PT, Sharpe RM, Smith LB. 2011. Smooth muscle cell-specific knockout of androgen receptor: A new model for prostatic disease. Endocrinology 152:3541–3551.
Wong YC, Tam NN. 2002. Dedifferentiation of stromal smooth muscle as a factor in prostate carcinogenesis. Differentiation 70:633–645.
Yu J, Akishita M, Eto M, Ogawa S, Son BK, Kato S, Ouchi Y, Okabe T. 2010. Androgen receptor-dependent activation of endothelial nitric oxide synthase in vascular endothelial cells: Role of phosphatidylinositol 3-kinase/akt pathway. Endocrinology 151:1822–1828.